Technical Note
radphi-1998-901

Prospects for running Radphi at design luminosity

Richard Jones
University of Connecticut, Storrs, CT

October 9, 1998

Abstract

The Radphi experiment relies on running an efficient trigger for all-neutral decay modes of the $\phi(1020)$ meson in the presence of significant electromagnetic and charged hadronic backgrounds. Experience during commissioning has shown that of the two, the former is by far the most serious limitation faced by the experiment. Calculations based upon data from early beam tests in 1997 indicated that the experiment would saturate in terms of its trigger efficiency over an order of magnitude below the flux needed to achieve the sensitivity required by the physics. The situation was subsequently improved by installation of a helium bag and shielding, and during 1998 commissioning the situation was reassessed by careful measurements. This report details the analysis of these data in terms of a mathematical model for our electronics, along with checks that verify the model. It also shows what improvements will be required to approach the efficiency demanded in order to run effectively near the design beam flux of $5 \cdot 10^7$ photons/s, and suggests a surprising simplification to our trigger that would achieve this end.

This note is divided into two parts. The first describes the formulae that are being used to model the experimental rates and compares them with measurements as a test of their validity. The second is concerned with how the model extrapolates to the beam intensities at which the experiment was designed to run, and what should be done to optimize the trigger for efficient operation under these conditions.

1 The model

All rates in the model are treated as functions of the beam intensity. The inputs to the model are the event fractions and the gate widths. Event fractions describe how the set of all possible triggers are divided into different classes based upon the kind of physical interaction that produced them. The gate widths are the effective duration of the signals that are used to form the trigger. At first it was assumed that the tagger-OR signal would be proportional to the beam intensity, but that was observed online to be incorrect, as described below. Instead the electron beam current, as measured at the Hall B beam dump, was taken as the beam intensity measurement. Although there is some uncertainty associated with this figure, at least it is believed to be linear over the full operating range of the tagger.

The level 0 trigger is a Boolean relation between OR signals from the recoil proton detector (RPD), charged particle veto (CPV) and the tagger. The first task in calibrating the model is to fit the measured scaler rates for each of these primitive OR's.

1.1 the tagger OR

What we call the *tagger OR* is a logical OR of the 19 discriminators monitoring the left-side phototubes on the top 19 tagger focal plane paddles. Each input to the OR generates an edge-triggered internal pulse of fixed duration; these are continuously OR'ed together to produce a single signal that we call the tagger OR. Note that this is different from what CLAS calls the tagger OR. The pulse duration is manually adjustable in the tagger electronics racks. In this model it is currently ignored (set to zero). The parameters in the model that concern the tagger are the linear slope r_T of the tagger OR in counts per nA, the tagging coincidence window width t_T and the scaler dead time d_T. The linear slope is the proportionality constant between beam current and the tagger OR rate in the linear region at low intensities.

In the model, every signal in the Radphi detector arises either from the interaction of a tagged photon (or its prompt reaction products) or it does not. These two are called *trues* and *accidentals* in the following discussion. By a tagged photon is meant a bremsstrahlung photon that was generated in the same electromagnetic cascade that contained an electron which produced a pulse over discriminator threshold in the left side of one of the tagger focal plane counters. The distinction between trues and accidentals is in the physics of the event that caused them, not in the temporal proximity of the tagger and detector signals, although the above restriction to *prompt* reaction products excludes trues where the two signals are separated by hundreds of nanoseconds. At finite rates it is practically impossible to distinguish trues from accidentals on an event-by-event basis. Nevertheless, as long as the events are independent, the two categories of events are distinct from each other and can be treated as two separate populations, to be added together in the end.

The content of the model is embodied in the following three formulae.

$$S_T = r_T I\, e^{-d_T\, r_T\, I} \tag{1}$$
$$\mathcal{F}_{acc.} = 1 - e^{-t_T\, r_T\, I} \tag{2}$$
$$\mathcal{F}_{true} = 1 \tag{3}$$

where S_T is the rate observed in the scaler counting the tagger OR signal and $\mathcal{F}_{true}$ [$\mathcal{F}_{acc.}$] is the probability that a true [accidental] hit in the detector will occur in coincidence with the tagger OR signal, within the tagging coincidence window t_T. There are some restrictions built into the model.

1. Beam current I must be high enough that the singles rates in the tagger phototubes can be ignored. The contribution from dark current should be less than 1% for I above a few nA.

2. The tagging counter discriminator dead time, together with the internal pulse duration in the module that forms the tagger OR, have been ignored. With the widths set to reasonable values, these effects are small compared with those which have been included in the model because they enter multiplied by the rate in a single tube (a couple MHz at most) rather than by the full tagger OR rate, in contrast to t_T and d_T. If they were to be included explicitly then the two-pulse resolving power of the tagger would also have to be included. At a rate of 2MHz per tagging counter and a 20ns discriminator gate

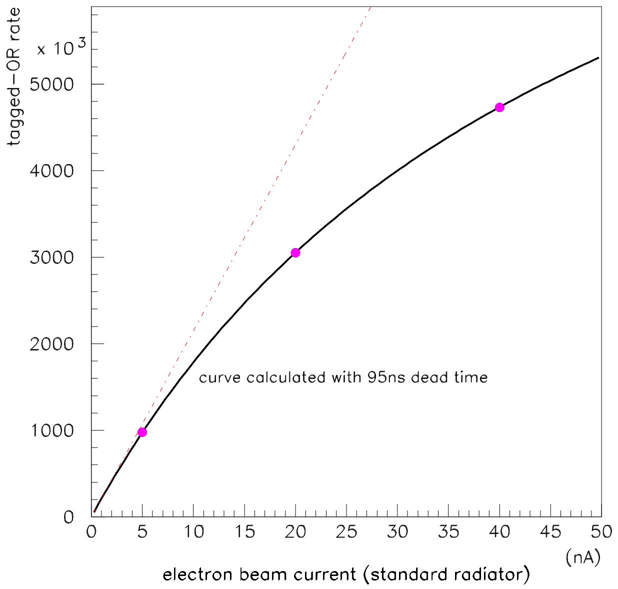

Figure 1: Tagger OR scaler rate *vs.* beam current measured at the beginning of the June run period.

width, tagger electronics dead time depresses the tagger OR by about 4%. At present the stability of our beam current measurement is no better than that.

3. It is assumed that beam factors that affect tagger performance, such as beam tune and steering, are constant so that r_T can be treated as a constant. For the set of runs throughout the June 1998 commissioning period that were used for this study, this assumption was upheld to within 2%.

4. It is assumed that the tagging coincidence window width t_T is wide enough to contain the entire coincidence peak. This assumption is implied by Eq. 3. For a well-timed setup this should be satisfied for t_T of 6ns or greater.

The parameters r_T and d_T were extracted from a two-parameter fit of measured tagger OR rates *vs.* beam current taken during the June run. The results from a scan taken early in the run are shown in Fig. 1. The dotted line shows the linear extrapolation with r_T from low rates. The saturation of the measurements gives a value for the scaler dead time d_T of 95ns. This large dead time is completely out of line with the specification for the scaler (200MHz), and indicates that there is an additional dead time hidden somewhere in the system that is not in the model. It turned out that the tagger discriminator widths had not been properly set. When this was done, a new scan produced the data shown in Fig. 2, now shown all the way out to 200nA. A new fit yields 10ns for d_T, which is in good agreement with the width of the tagger OR pulse width seen on the oscilloscope. Although the model is merely descriptive at this point, getting reasonable values for the parameters provides a good check that the electronics is working as expected.

1.2 the RPD OR

The rates in the recoil proton detector are about two orders of magnitude smaller than in the tagger, whereas the time scale for the electronics is the same. Therefore all dead time effects in the circuits that produce the RPD OR are ignored. Logically the RPD OR is more complicated than the tagger OR: it is composed in the following way. First each of the 12 thick (E) counters is AND'ed with its corresponding thin (G) counter, then these 12 coincidence signals are combined together in an OR. The width of the coincidence gate is ignored (set to zero) in the model, and the rate is a linear function of the beam current.

$$S_R = r_R \, I \tag{4}$$

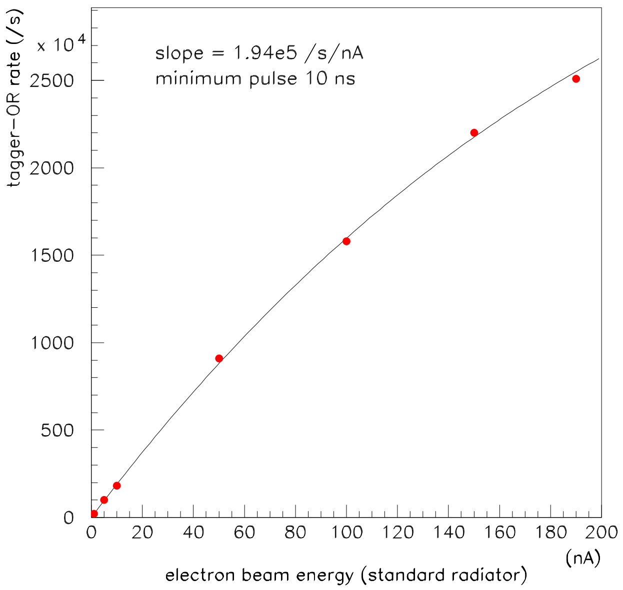

Figure 2: Tagger OR scaler rate *vs.* beam current measured at the end of the June run period.

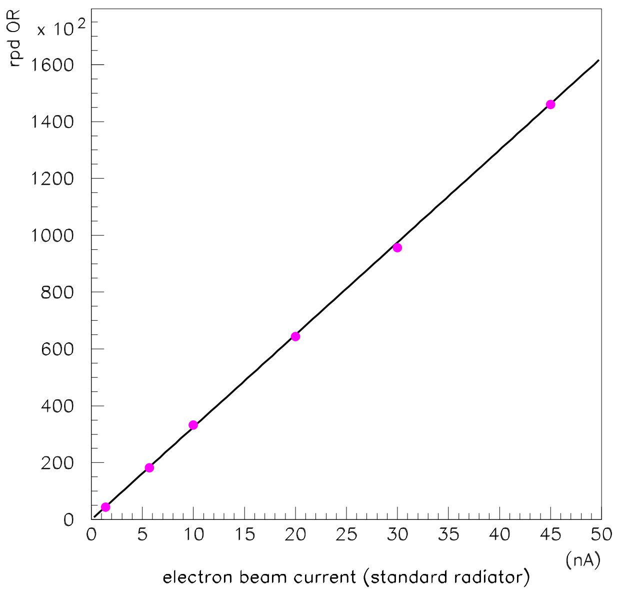

Figure 3: RPD OR scaler rate *vs.* beam current measured at the beginning of the June run period.

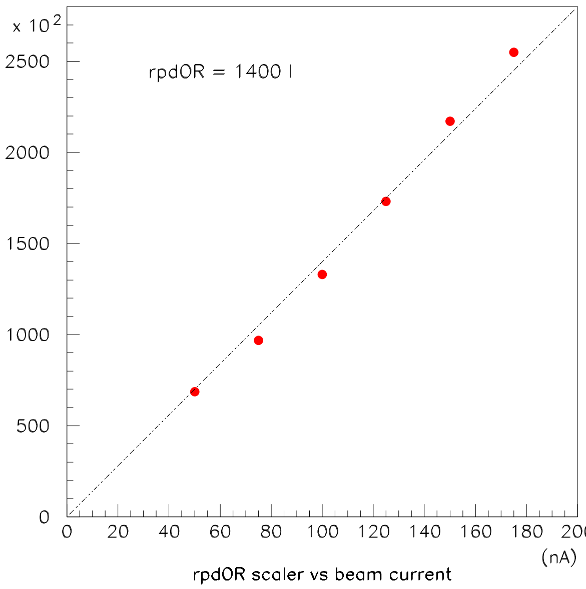

Figure 4: RPD OR scaler rate *vs.* beam current measured at the end of the June run period.

where S_R is the scaler monitoring the RPD OR signal and r_R is the proportionality constant between the RPD OR and the beam current.

The value of r_R varied significantly during the run, depending in particular on the threshold and gains in the RPD counters, and to some extent on the quality of the beam tune. The difference between scans taken at the beginning of the June period and the end can be seen by comparing Fig. 3 with Fig. 4. The decrease in slope by a factor of 2.5 is mainly due to raising the RPD discriminator threshold. The deviation from a straight line during the high-current scan in Fig. 4 is due to changing beam conditions during that scan; CLAS emptied and refilled their target during this scan. The effect of the CLAS target is much more apparent in the UPV rate, shown below. The principal restriction on this part of the model is that the RPD rate must not exceed the level where electronics dead times begin to be important, around 5-10MHz in the OR. Given that this corresponds to 10^9 tagged photons/s, this part of the model is free of restrictions.

1.3 the UPV OR

The rates in the upstream veto wall run a factor of 20-40 lower than the tagger OR. The UPV OR is formed by a OR'ing together the outputs from the 8 discriminators connected to the UPV counters. The width t_C of the UPV OR signal is assumed to be the same as that of the CPV. The observed scaler rate S_U for the UPV OR is given in the model by

$$S_U = r_U \, I \tag{5}$$
$$\mathcal{F}_{Uhit} = 1 \tag{6}$$
$$\mathcal{F}_{Umiss} = 1 - e^{-t_C \, r_U \, I} \tag{7}$$

where r_U is the rate in the UPV OR per nA of beam current. The value of r_U varied by as much as a factor of 5, depending upon the quality of the beam tune and what CLAS was doing. The scan shown in Fig. 5 taken towards the beginning of the June period under average beam conditions should be contrasted with the scan shown in Fig. 6 during which CLAS emptied their hydrogen target. Under no circumstance did the UPV OR rate rise high enough that nonlinear effects from electronics dead time became observable. This implies a restriction on the validity of the model to rates where the UPV OR is below 5-10MHz. Under worst-case conditions this implies a maximum beam current of 360nA, well above our design luminosity that corresponds with this radiator to 250nA. The other restriction of the model is that the veto window width is

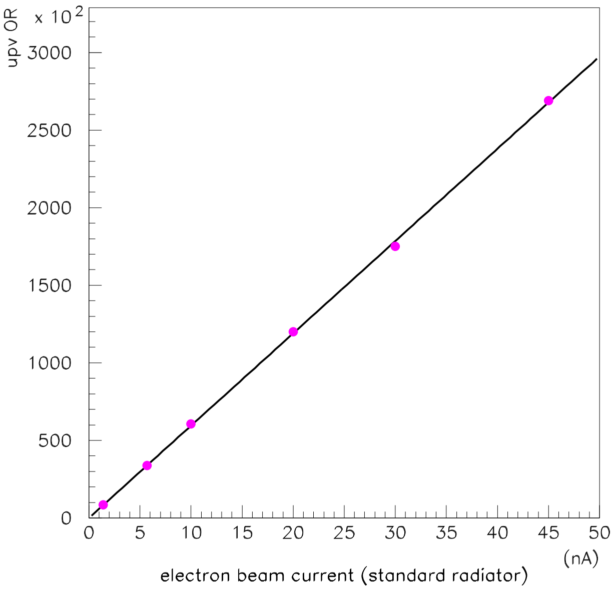

Figure 5: UPV OR scaler rate *vs.* beam current measured at the beginning of the June run period.

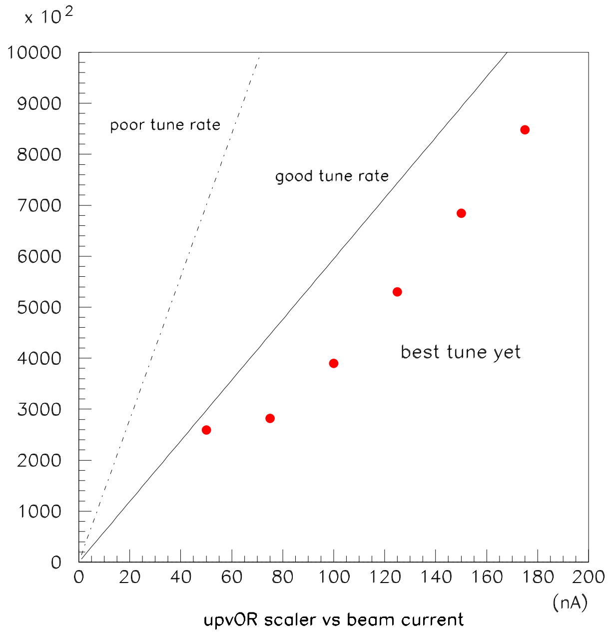

Figure 6: UPV OR scaler rate *vs.* beam current measured at the end of the June run period.

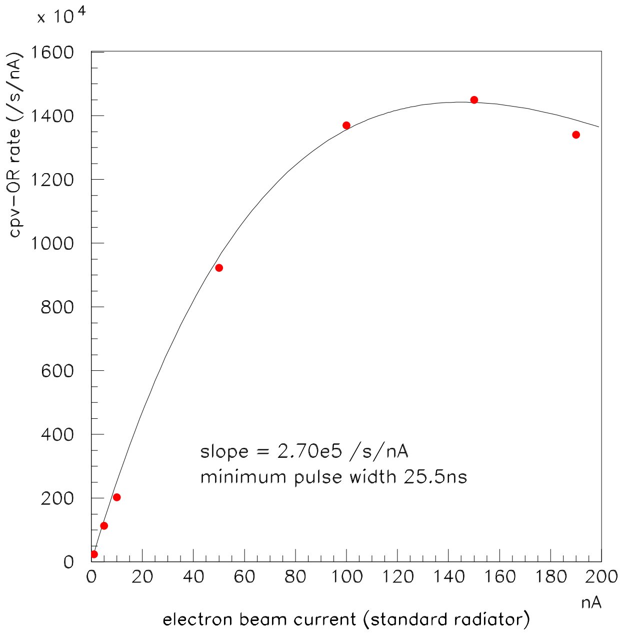

Figure 7: CPV OR scaler rate *vs.* beam current measured at the beginning of the June run period.

wide enough to exclude the entire coincidence peak (see Eq. 6), which implies a lower limit on $t_{_C}$ of roughly 15ns (see Fig. 18 below).

In analogy with the classification of events as either trues or accidentals with respect to the tagger, each event is also classified as either a *Uhit* or *Umiss* event, depending upon whether or not whatever produced the hit in the RPD shared the same mother photon as something that produced a hit over threshold in the UPV. The quantities $\mathcal{F}_{Uhit}$ $[\mathcal{F}_{Umiss}]$ represent the fractions of events in each class which fall within the UPV coincidence window. As before, one assumes in the definition of Uhit events that the causal chain connecting the RPD and UPV hits is a few tens of ns long at most.

1.4 the CPV OR

The charged particle veto wall is the component of Radphi that encounters the highest rate, and so is the most sensitive part of our apparatus to dead-time effects. It is important, therefore that the model correctly describe the behavior of the logic that generates the CPV OR. Similar to the UPV logic, the CPV OR is formed by discriminating the individual signals from the 29 phototubes, producing for each a train of logic pulses of fixed duration and then OR'ing these signals together. The formulae which embody the model are as follows.

$$S_{_C} = r_{_C}\, I\, e^{-d_{_C}\, r_{_C}\, I} \tag{8}$$

$$\mathcal{F}_{Chit} = 1 \tag{9}$$

$$\mathcal{F}_{Cmiss} = 1 - e^{-t_{_C}\, r_{_C}\, I} \tag{10}$$

where the symbols $S_{_C}$, $r_{_C}$, $d_{_C}$, $t_{_C}$ and $\mathcal{F}_{Chit}$, $\mathcal{F}_{Cmiss}$ have the usual meanings. As in the case of the tagger OR, a distinction is made between the coincidence window width $t_{_C}$ and the scaler dead-time $d_{_C}$ although the two are substantially determined by the same quantity, the width of the CPV OR pulse generated by the OR module. The scaler dead-time contains whatever additional dead-time is inherent in the scaler, whereas the coincidence gate width contains corrections due to the minimum overlap required to generate a valid veto, so the two are not exactly the same. However they should both be close to the CPV pulse width measured on the oscilloscope, and this provides an important check that the electronics is working as expected.

The results of a scan taken towards the beginning of the June period is shown in Fig. 7. The tendency of the CPV OR scaler to decrease at high rates is due to the fact that the scaler is counting the transitions

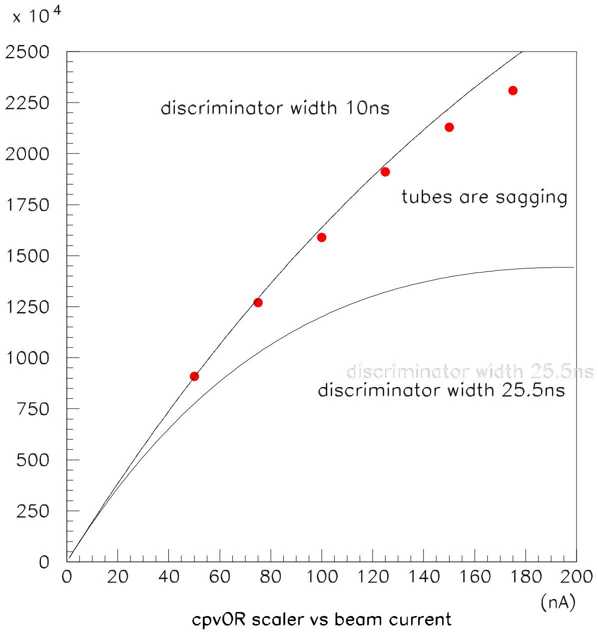

Figure 8: CPV OR scaler rate *vs.* beam current measured at the end of the June run period.

between 0 and 1 in the CPV OR signal and not the amount of time it is on or off. At very high rates one expects the scaler to go to zero (the CPV OR is always 1) which is the limit of Eq. 8 at high rates. The two-parameter fit to the data in Fig. 7 gives a fairly precise value of 25.5ns for d_C, which disagrees with the value of 10ns that was programmed into the OR module for its gate width. Upon examination, it was discovered that the discriminator modules had been operating in updating mode, which extends the width of the CPV OR signal to however long the pulse remains over threshold. A later scan shown in Fig. 8 gives a more consistent value of 10ns for d_C, indicating that the problem was fixed. Once more the model correctly diagnosed a subtle bug in the electronics and produced consistent results after the bug was fixed.

There are still significant deviations from the expected model behavior for the high-rate points in Fig. 8. One possibility is that it is due to CLAS emptying their target during that scan. A slight effect due to this is observable in these data: compare the U-shaped nonlinearity in the low-rate points in Fig. 6 with the corresponding points in Fig. 8. However the suppression at high rates goes beyond what would be expected based upon a comparison between those two figures (the data were taken during the same scan). The observation that the adc spectra from the central CPV counters showed a marked decrease in gain for the high-rate points taken during this scan indicates that some of the CPV tubes are showing signs of saturation.

The most important restriction on the validity of this model arises from its ignoring the effects of discriminator dead-time at the level of the individual counters. All of the observations made above under the tagger section apply here as well. Because the rates in the individual channels are limited to a few MHz, dead-time effects are much less important there than they are once one is working with the OR signal. Nevertheless losses at the level of 5% can be expected from this source for those tubes running at 5MHz under full design intensity. In order to take these losses into account consistently, one must also bring in the two-pulse resolving power of these tubes and electronics, which must be measured. At present the stability of the beam current measurement is not sufficient to measure dead-time effects a level better than 5%. In the present model they are being ignored (set to zero). The restriction $t_C \geq 15$ns discussed under the UPV section above also applies here as a condition for the validity of Eq. 9

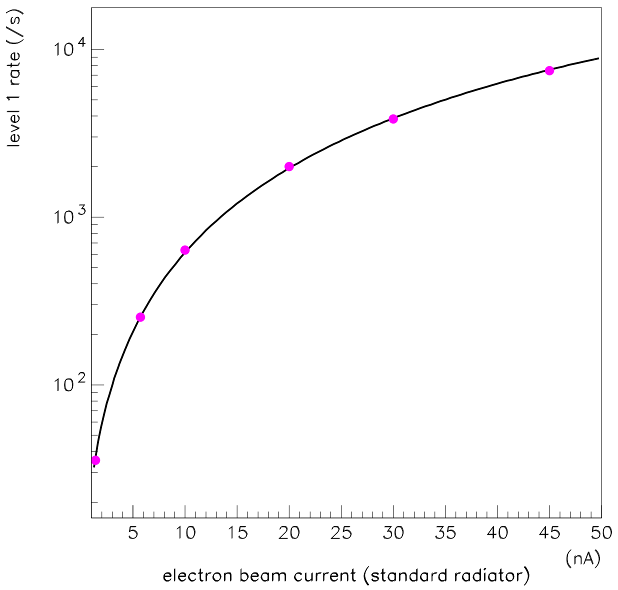

Figure 9: Level 0 scaler rate *vs.* beam current measured at the beginning of the June run period.

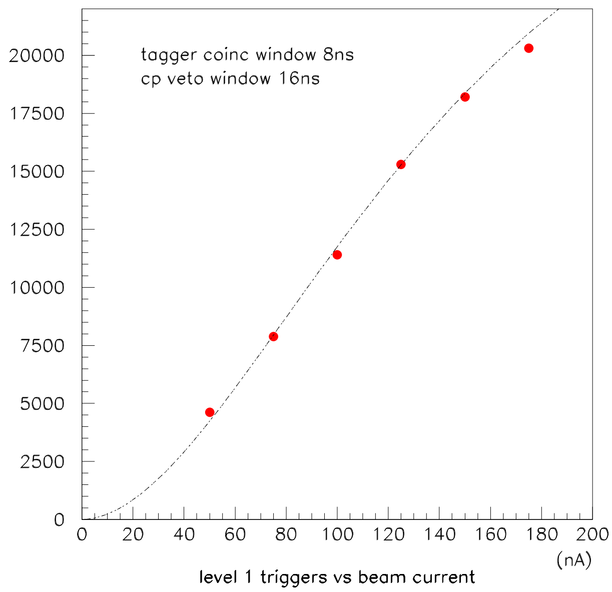

Figure 10: Level 0 scaler rate *vs.* beam current measured at the end of the June run period.

1.5 the level 0 trigger

The level 0 trigger is what generates the gate for the adc and tdc modules. The logic formula embodied in our present level 0 circuit is as follows.

$$L_0 \;=\; \mathrm{RPD} \,\cap\, \mathrm{TAG} \,\cap\, \overline{(\mathrm{CPV} \cup \mathrm{UPV})} \tag{11}$$

With the above calibrated model for the constituent signals, it should be possible to generate a prediction for the level 0 trigger rate. However there is some additional information that still must be supplied as input to the model, that is, the fraction of the total RPD OR rate that comes from *trues* $\cap$ *Umiss* $\cap$ *Cmiss* events. Let the intersection of Umiss and Cmiss sets be called *noCP* and the intersection of the trues and noCP sets be called *signal*. Not all *signal* events are interesting from the physical point of view, but they are the fish that this trigger has been designed to catch. Under conditions of low beam intensity, only signal events produce level 0 triggers. At high rates two things happen: signal events are lost, and non-signal events are picked up. Presumably higher level triggers and offline analysis will be able to discard the non-signal events, or at least subtract them away statistically, but the lost signal is a more serious problem; those events are gone forever. Let f_n designate the fraction of the RPD OR rate that is noCP and let f_s represent the fraction that is signal. Then

$$\begin{aligned} S_{0} &= r_{R}\, I\, f_s\, \mathcal{F}_{true}(1-\mathcal{F}_{Umiss})\,(1-\mathcal{F}_{Cmiss}) + \\ &\quad\; r_{R}\, I\, (f_n - f_s)\mathcal{F}_{acc.}(1-\mathcal{F}_{Umiss})\,(1-\mathcal{F}_{Cmiss}) \end{aligned} \tag{12}$$

$$R_{0} = \frac{S_{0}}{1 + S_{0}(d_2 + \mathcal{F}_2\, d_{DAQ})} \tag{13}$$

where S_0 is the rate observed in a free-running scaler monitoring the level 0 logic signal and R_0 is the rate of level 0 triggers after the level 0 signal has been gated by the busy signal. The busy signal is present during level 2 processing (duration d_2) and during event readout (duration d_{DAQ}) for events passed by level 2. The fraction $\mathcal{F}_2$ of level 0 triggers that are passed by level 2 is defined in the next section. The input parameters in the model are always represented by lower-case letters.

A comparison between the model and observations of S_0 made towards the beginning and the end of the June period is shown in Fig. 9 and 10, respectively. Fig. 10 shows how complicated the shape is over the range of the scan. The linear region at low current transitions around 10nA to a quadratic behavior due to accidental coincidence with the tagger. Then above 50nA the quadratic rise stops and the curve turns over as the accidental charged-particle vetoes begin to suppress the trigger rate. The parameters that control the shape of this curve are t_T, t_C, f_n and f_s; the first two were varied to fit the measured S_0 data whereas f_s and f_n were measured independently during runs taken with special triggers. The agreement between the values for t_T and t_C with what is seen on the oscilloscope indicates that the electronics is behaving as expected. Note that t_T is expected to be a few ns less than the tagger OR pulse width because a few ns of overlap with the RPD OR signal is required before a coincidence is registered. Likewise t_C should be few ns less than the sum of the CPV OR and RPD OR pulse widths because only a few ns of overlap between the two is sufficient to generate a veto. This implies a practical minimum value on the effective veto window width of 8-10ns given that one is working with a minimum width around 5ns for the CPV OR and RPD OR signals.

The only new restriction that appears in the model at this level is that Eq. 12 implicitly assumes that the UPV OR and CPV OR signals are statistically independent. This is the assumption behind the factorization of the accidental veto probability into the product $(1-\mathcal{F}_{Umiss})(1-\mathcal{F}_{Cmiss})$. These two signals are certainly not independent because many tracks passing through the UPV will also create a signal in the CPV. However the UPV OR rate is so low that it makes very little practical difference how random UPV vetoes are accounted for in the model. At the other extreme one could assume that every UPV OR hit is accompanied by a CPV OR signal, in which case the factor $(1-\mathcal{F}_{Umiss})$ in Eq. 12 should be replaced by unity. At the full operating intensity of 250nA this increases the value of S_0 by roughly 2%.

1.6 the level 2 trigger

The level 2 trigger processor makes a fast estimate of the total energy in the lead glass wall and applies a threshold cut on this quantity. Presumably the signal events are more likely to contain a large neutral dose than nonsignal events. It is described within the model by the following formula,

$$\mathcal{F}_2 = \frac{f_{2s}\, f_s\, \mathcal{F}_{true} + f_{2n}\,(f_n - f_s)\,\mathcal{F}_{acc.}}{f_s\, \mathcal{F}_{true} + (f_n - f_s)\,\mathcal{F}_{acc.}} \tag{14}$$

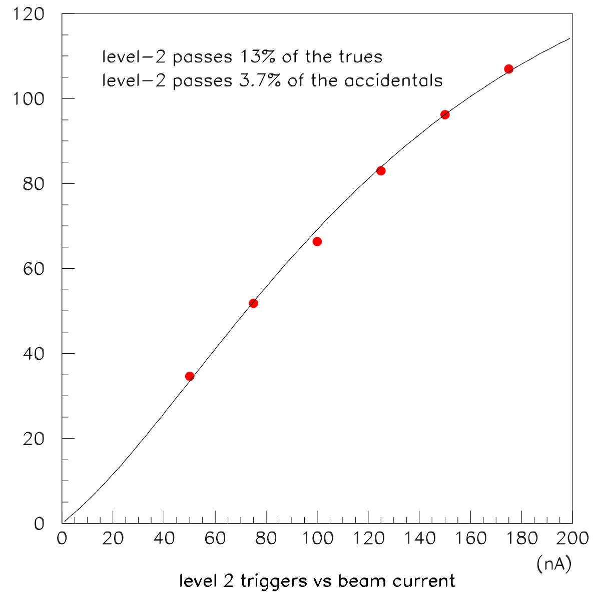

Figure 11: Level 2 scaler rate *vs.* beam current measured at the end of the June run period.

where the input parameters f_{2s} and f_{2n} are the level 2 pass fractions for level 0 triggers (noCP events) that are signal (*i.e.* trues) and nonsignal (*i.e.* accidentals) respectively. The data overlayed with the model fit are shown in Fig. 11 for the scan taken at the end of the June period. If the level 2 processor is doing its job then one would expect that $f_{2s} \gg f_{2n}$ which is what is observed.

1.7 yield of all-neutral hadronic events

As has been shown in the previous sections, the model gives a good description of the full set of counting rates of relevance to our trigger from very low intensities up to the beam current at which Radphi has been designed to operate. The model now permits a decomposition of the event sample collected at any given beam intensity into signal and background components, and to compare the efficiency for signal collection at various beam currents. The rate at which signal events are recorded on tape, denoted S_S, is given by

$$S_S = r_R \, I \, f_s \; \mathcal{F}_{true}(1 - \mathcal{F}_{Umiss})\,(1 - \mathcal{F}_{Cmiss})\, f_{2s} \left(\frac{R_0}{S_0}\right) \tag{15}$$

which is to be compared with the corresponding rate for an experiment without any dead-time effects, S_I,

$$S_I = r_R \, I \, f_s \, f_{2s} \tag{16}$$

which is directly proportional to the beam intensity. The situation at the end of the June period is summarized in Fig. 12. In particular, it shows that increasing the beam current above 100nA does very little to increase the rate at which signal is being written to tape; in fact above 175nA it begins to decrease. Given that the proposal assumed no dead-time effects and an intensity that corresponds to 250nA on this figure, we are presently a factor of 4 short of our design goal in terms of rate capability.

Given that no single stage of the electronics or data acquisition chain was operating near its maximum rate (the phototubes and bases on the CPV were running near their limit but they do not contribute dead-time within this model) there is good reason to be skeptical that the overall losses are so high. As a check on this result, Scott Teige analyzed the data from the intensity scan taken at the end of the June period, and extracted the yield of η and ω mesons from their 2γ and 3γ decays respectively. The yields are plotted as a real-time rate in Figs. 13-14. The solid curves are the shape of the signal (red) curve from Fig. 12. Fig. 13 in particular gives striking confirmation of the model prediction.

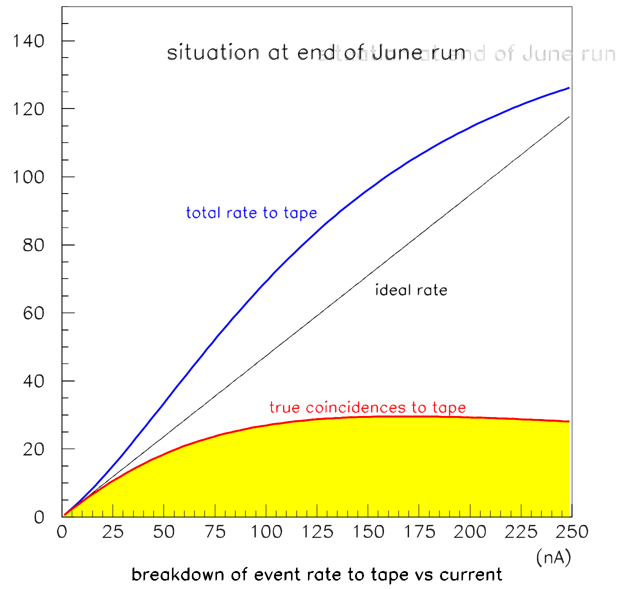

Figure 12: Comparison between ideal and actual rates of recording signal events on tape as a function of beam intensity, evaluated by the model under the conditions at the end of the June 1998 run period.

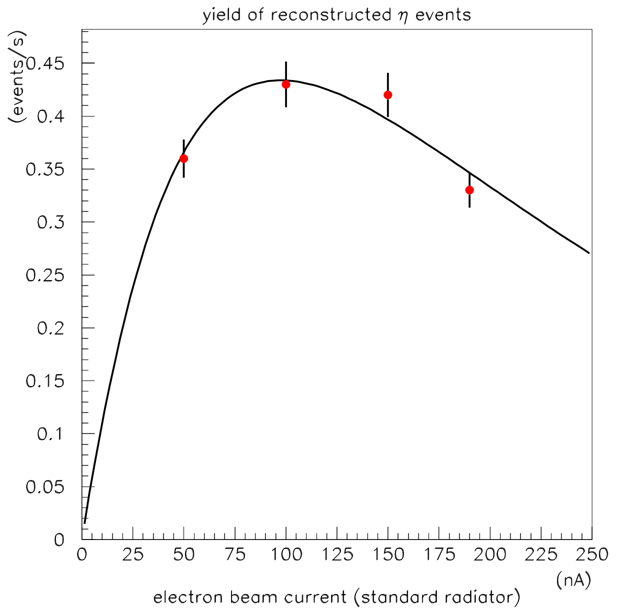

Figure 13: Comparison between ideal and actual rates of recording signal events on tape as a function of beam intensity, evaluated by the model under the conditions at the end of the June 1998 run period.

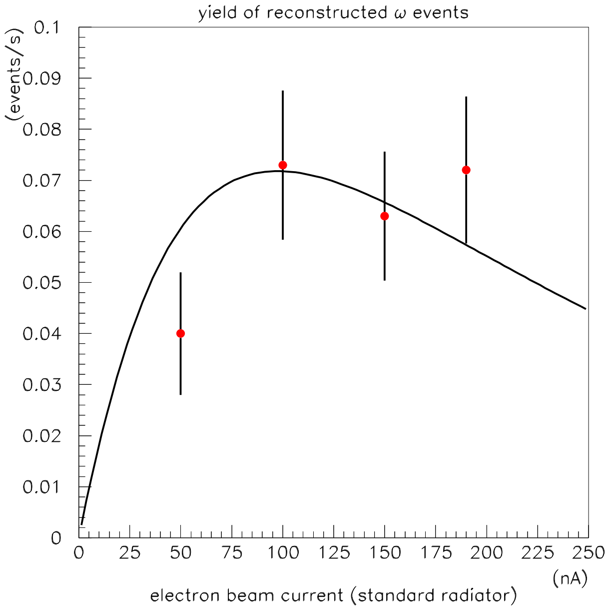

Figure 14: Comparison between ideal and actual rates of recording signal events on tape as a function of beam intensity, evaluated by the model under the conditions at the end of the June 1998 run period.

2 An optimized trigger for 1999

2.1 the current situation

Supposing then that the model is giving correct results, what part of the electronics chain is producing the majority of the losses? The answer to this question is illustrated in Fig. 15. Depending upon what value one takes for the width of the CP veto window, the losses are shared more or less equally between random CP vetoes and dead-time associated with the level 2 processor, with data acquisition contributing an additional 10-15%. Recall that there is a restriction on the validity of the model that $t_C \geq 15$ns. Reducing t_C below this bound will introduce a leak in the CP veto and cause the losses from the level 2 processor and DAQ to increase faster with decreasing veto window width than is shown in the plot. Fig. 15 actually includes extra losses at level 2 from some broken adc channels that generated significant processing overhead during the June period, which explains why this figure looks somewhat worse than the situation at 250nA in Fig. 12 where the broken channels have been removed. Nevertheless the conclusion from this figure is correct that the CP veto and the level 2 processor are primarily responsible for the losses in our present setup.

A complete list of the model inputs used to generate the figures in this section is given in Table 2.1. Many of these numbers changed as timing, thresholds and gains were adjusted throughout the run period. A few were sensitive to the quality of the beam tune. The numbers given in the table are the ones that describe the situation during the intensity scan taken at the end of the June period.

2.2 upper-level trigger improvements

From Fig. 15 it is seen that level 2 processor dead-time is a leading source of loss in our system. Several people have suggested that this loss could be reduced by a pre-level-2 decision based simply upon a count of lead glass blocks over some threshold. This idea was tested, first by Phil Rubin and then by Elton Smith and Kyle Burchesky[1], using data collected during the June period. The conclusion is that this simple criterion rejects 95% or more of the level 0 triggers, while preserving almost all of what the level 2 processor would keep. In Table 1 of their report, Elton and Kyle show that for a particular choice of threshold, more than 97% of the level 0 triggers are rejected while 98% of the events with MAM values of 64 or higher (the level 2 threshold used during the June period) are preserved.

The way that this would work is as follows. The adc modules connected to the lead glass detector

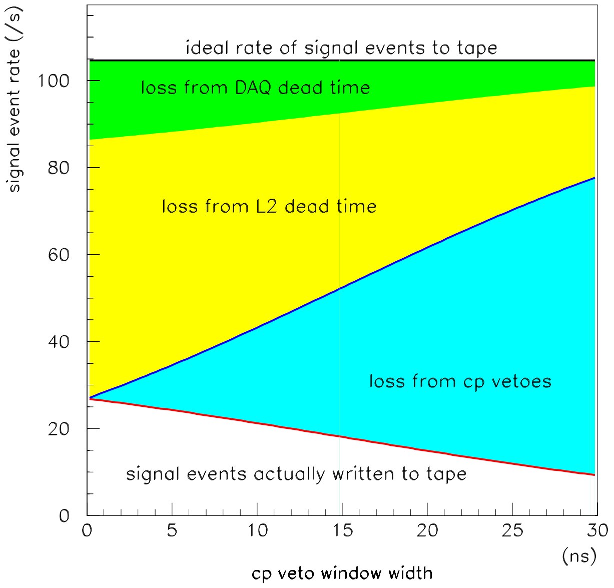

Figure 15: Decomposition of signal losses among various stages of the event pipeline as a function of the width of the CPV veto window t_C at a beam intensity close to the maximum point in the scan taken at the end of the June period. Values of t_C below 15ns represent an extrapolation of the model beyond its range of validity because in that regime the CP vetoes cannot be treated as fully efficient.

Table 1: Parameters supplied as input to the model, together with information about how the value for the parameter was obtained.

parameter	value		method
r_T	$1.94 \cdot 10^5$	/s/nA	fit to scaler data
r_R	$1.45 \cdot 10^3$	/s/nA	fit to scaler data
r_U	$1.4 \cdot 10^4$	/s/nA	fit to scaler data
r_C	$2.7 \cdot 10^5$	/s/nA	fit to scaler data
t_T	$1.4 \cdot 10^{-8}$	s	fit to scaler data
t_C	$1.2 \cdot 10^{-8}$	s	fit to scaler data
d_T	$1.0 \cdot 10^{-8}$	s	fit to scaler data
d_C	$1.0 \cdot 10^{-8}$	s	fit to scaler data
d_2	$1.4 \cdot 10^{-5}$	s	measured on scope
d_{DAQ}	$6.7 \cdot 10^{-4}$	s	measured on scope
f_s	$2.6 \cdot 10^{-3}$		measured at low rates
f_n	$5.5 \cdot 10^{-1}$		measured with veto in/out
f_{2s}	$1.3 \cdot 10^{-1}$		fit to scaler data
f_{2n}	$3.5 \cdot 10^{-3}$		fit to scaler data

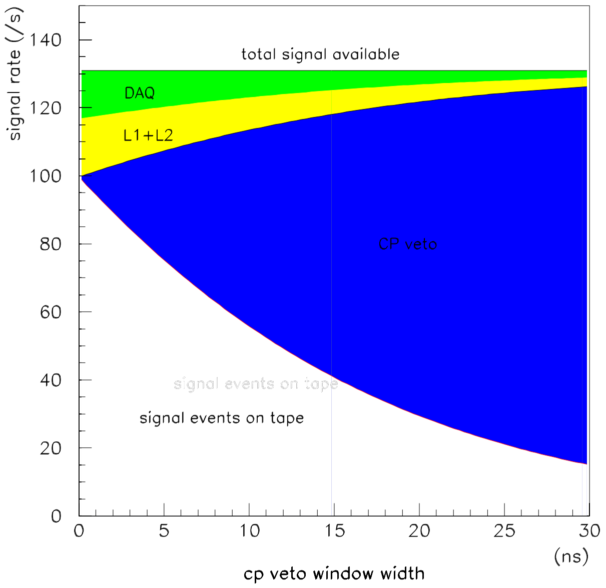

Figure 16: Decomposition of signal losses among various stages of the event pipeline as a function of the width of the CPV veto window t_C at a beam current of 250nA, with the upper-level trigger improvements foreseen for 1999 running in place. Values of t_C below 15ns represent an extrapolation of the model beyond its range of validity because in that regime the CP vetoes cannot be treated as fully efficient.

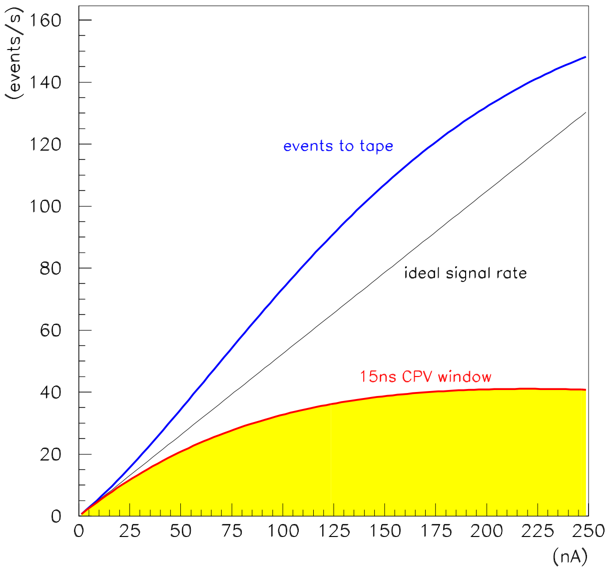

Figure 17: Comparison between ideal and actual rates of recording signal events on tape as a function of beam intensity, under the conditions of a level 1 trigger and improved DAQ foreseen for 1999 running.

produce a logic signal on the Fastbus auxiliary backplane a short time after the integration gate has closed. This signal is the output of a comparator between the charge on the integrator for that channel and some programmable level. A fast OR of the outputs from all instrumented blocks in the wall could be formed, and a fast-clear could be formed if the OR signal is absent. Those familiar with the adc say that it could be ready for the next event as soon as 250ns after the fast-clear is received. The LeCroy 1877 multihit tdc specification gives 290ns as the required fast-clear settling time, but the 1875A high-resolution tdc that we use the digitize the tagger and RPD signals requires 950ns between the fast-clear and the earliest subsequent gate. Therefore the earliest that the acquisition could be re-enabled following a fast clear from a level 1 decision would be $1.2\mu s$ from the receipt of the level 0 trigger. This is equivalent to a 10-fold reduction in the level 2 dead-time.

In order to incorporate this improvement into the model, it is necessary to break up the level 1 passing fraction $\mathcal{F}_1$ of 97% into a passing fraction for signal and a part for nonsignal, similar to how it was done in Eq. 14 for $\mathcal{F}_2$.

$$\mathcal{F}_1 = \frac{f_{1s}\, f_s\, \mathcal{F}_{true} + f_{1n}\,(f_n - f_s)\,\mathcal{F}_{acc.}}{f_s\, \mathcal{F}_{true} + (f_n - f_s)\,\mathcal{F}_{acc.}} \tag{17}$$

The data in Ref. [1] were taken at beam intensities where the triggers were more than 95% nonsignal, therefore the value of 3% that they report for $\mathcal{F}_1$ is essentially a determination of f_{1n} and leaves f_{1s} unconstrained by the data. In what follows I have been conservative and set f_{1s} to 1. While it is surely an overestimate to say the every signal event has at least one large hit in the LGD, at the beam intensities of interest for this model it makes very little difference to the dead-time what value is used for f_{1s}.

Another area where losses may be reduced is in the data acquisition dead-time. Phil Rubin and David Abbott have found a way to reduce the time it takes to read out and store an event from the 670μs observed during 1998 running to less than 300μs. Being cautious, I have taken 300μs as the new estimate for readout dead-time per event $d_{_{DAQ}}$. With the level 1 trigger and data acquisition speed-up taken into account, instead of Fig. 15 we now have Fig. 16. Fixing the value of $t_{_C}$ at 15ns (minimum value for a fully efficient veto), the yield of signal *vs.* beam intensity is shown in Fig. 17. A significant improvement has been obtained over the situation in 1998 shown in Fig. 12 but we are still not in a position to make effective use of beams much over 150nA.

2.3 running without the CP veto

From Fig. 16 it is clear that to make further progress in reducing our electronics dead-time we have no choice but to compromise on our original wish for a online clean neutral trigger. The tdc spectrum for the CPV OR is shown in Fig. 18, taken during a run where the CP veto was removed from the trigger. All of the events in this sample passed the level 2 trigger condition. This figure shows that a veto window of 15ns is necessary in order to reject CP events online with full efficiency. Examination of the spectra for the individual counters shows that this peak width is essentially all coming from intrinsic time spread of the CP signals in the individual counters and not from timing misalignment.

There is no absolute reason why the CP veto must be done online. Several have suggested that we could reduce the width of the online CP veto window and accept a certain fraction of the CP events, and then reject them offline using the tdc data. The model presented above can be generalized to cover this possibility, albeit at the expense of some additional complication. Eq. 12 above takes on its simple form because it is assumed that CP events are completely rejected at all beam intensities (see Eqs. 6, 9). Relaxing this assumption turns the two terms of Eq. 12 into the eight terms of Eq. 18.

$$\begin{aligned} S_{_0} \;=\;\; & r_{_R}\, I\, f_{_{T\not C\not U}}\,(1-\mathcal{F}_{Cmiss})\,(1-\mathcal{F}_{Umiss})\,\mathcal{F}_{true} + \\ & r_{_R}\, I\, f_{_{\not T\not C\not U}}\,(1-\mathcal{F}_{Cmiss})\,(1-\mathcal{F}_{Umiss})\,\mathcal{F}_{acc.} + \\ & r_{_R}\, I\, f_{_{TC\not U}}\,(1-\mathcal{F}_{Chit})\,(1-\mathcal{F}_{Umiss})\,\mathcal{F}_{true} + \\ & r_{_R}\, I\, f_{_{\not TC\not U}}\,(1-\mathcal{F}_{Chit})\,(1-\mathcal{F}_{Umiss})\,\mathcal{F}_{acc.} + \\ & r_{_R}\, I\, f_{_{T\not CU}}\,(1-\mathcal{F}_{Cmiss})\,(1-\mathcal{F}_{Uhit})\,\mathcal{F}_{true} + \\ & r_{_R}\, I\, f_{_{\not T\not CU}}\,(1-\mathcal{F}_{Cmiss})\,(1-\mathcal{F}_{Uhit})\,\mathcal{F}_{acc.} + \\ & r_{_R}\, I\, f_{_{TCU}}\,(1-\mathcal{F}_{Chit})\,(1-\mathcal{F}_{Uhit})\,\mathcal{F}_{true} + \\ & r_{_R}\, I\, f_{_{\not TCU}}\,(1-\mathcal{F}_{Chit})\,(1-\mathcal{F}_{Uhit})\,\mathcal{F}_{acc.} + \end{aligned} \tag{18}$$

where I have used an obvious notation for the fractions f_{XXX} of the RPD OR rate that belong to each category. For example, $f_{_{\not TCU}}$ represents the fraction of RPD OR hits that were generated by a reaction

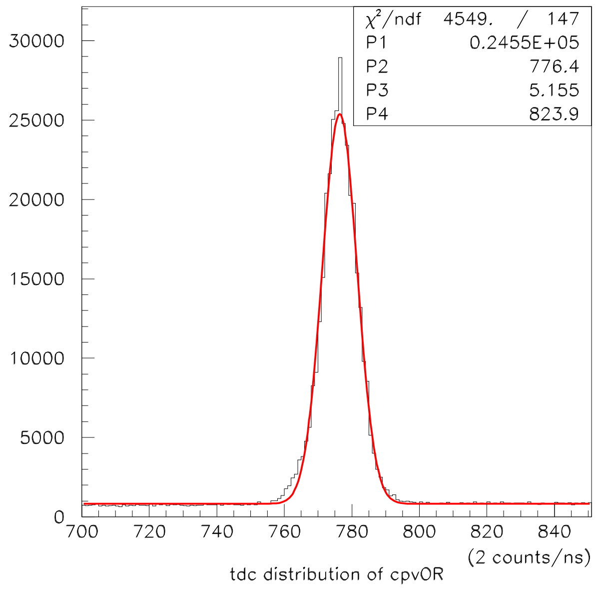

Figure 18: Coincidence peak in the tdc spectrum of the CPV OR for a run during the June period where the CP vetoes were removed from the trigger. The level 2 trigger was still present.

chain that also includes particles that produced hits over threshold in the CPV and UPV counters, but nothing over threshold in the left-side tagger readout. In Eq. 18 f_s is denoted $f_{T\not C\not U}$ and f_n is equivalent to $f_{T\not C\not U} + f_{\not T\not C\not U}$. Eq. 12 is simply the first two lines of Eq. 18; the subsequent lines enter as soon as $\mathcal{F}_{Uhit}$ and $\mathcal{F}_{Chit}$ deviate from unity.

Actually we have no reason to decrease the veto window width for the UPV OR, the problem is with the CPV OR. Therefore let $\mathcal{F}_{Uhit} = 1$. This gets rid of the last four lines of Eq. 18 and leaves only $f_{TC\not U}$ and $f_{\not TC\not U}$ as additional inputs to extend the range of applicability of the model to $t_C < 15$ns. The formula for $\mathcal{F}_{Chit}$ now becomes

$$\mathcal{F}_{Chit} = 2\left(1 - \mathrm{Erf}(\frac{t_C}{\sigma_C})\right) \tag{19}$$

where σ_C is the standard deviation of the CPV coincidence peak, 2.6ns in Fig. 18. Carrying on the generalization of the model to Eqs. 17,14 we obtain

$$\begin{aligned}\mathcal{F}_1 = \left(\frac{r_R\, I}{S_0}\right) [\ & f_{1_{T\not C\not U}}\, f_{T\not C\not U}\,(1-\mathcal{F}_{Cmiss})\,(1-\mathcal{F}_{Umiss})\,\mathcal{F}_{true} + \\ & f_{1_{\not T\not C\not U}}\, f_{\not T\not C\not U}\,(1-\mathcal{F}_{Cmiss})\,(1-\mathcal{F}_{Umiss})\,\mathcal{F}_{acc.} + \\ & f_{1_{TC\not U}}\, f_{TC\not U}\,(1-\mathcal{F}_{Chit})\,(1-\mathcal{F}_{Umiss})\,\mathcal{F}_{true} + \\ & f_{1_{\not TC\not U}}\, f_{\not TC\not U}\,(1-\mathcal{F}_{Chit})\,(1-\mathcal{F}_{Umiss})\,\mathcal{F}_{acc.}\ ]\end{aligned} \tag{20}$$

$$\begin{aligned}\mathcal{F}_2 = \left(\frac{r_R\, I}{S_0}\right) [\ & f_{2_{T\not C\not U}}\, f_{T\not C\not U}\,(1-\mathcal{F}_{Cmiss})\,(1-\mathcal{F}_{Umiss})\,\mathcal{F}_{true} + \\ & f_{2_{\not T\not C\not U}}\, f_{\not T\not C\not U}\,(1-\mathcal{F}_{Cmiss})\,(1-\mathcal{F}_{Umiss})\,\mathcal{F}_{acc.} + \\ & f_{2_{TC\not U}}\, f_{TC\not U}\,(1-\mathcal{F}_{Chit})\,(1-\mathcal{F}_{Umiss})\,\mathcal{F}_{true} + \\ & f_{2_{\not TC\not U}}\, f_{\not TC\not U}\,(1-\mathcal{F}_{Chit})\,(1-\mathcal{F}_{Umiss})\,\mathcal{F}_{acc.}\ ]\end{aligned} \tag{21}$$

where $f_{1_{XXX}}$ and $f_{2_{XXX}}$ are the level 1 and level 2 pass fractions, respectively, for level 0 event class XXX.

The input parameters for the model used to generate Figs. 19-21 are listed in Table 2.3. For some of the input values to the generalized model I had to make an educated guess. For example, $f_{TC\not U}$ is measured directly in a run with the UPV veto enabled but the CPV veto removed. It appears that we did not take

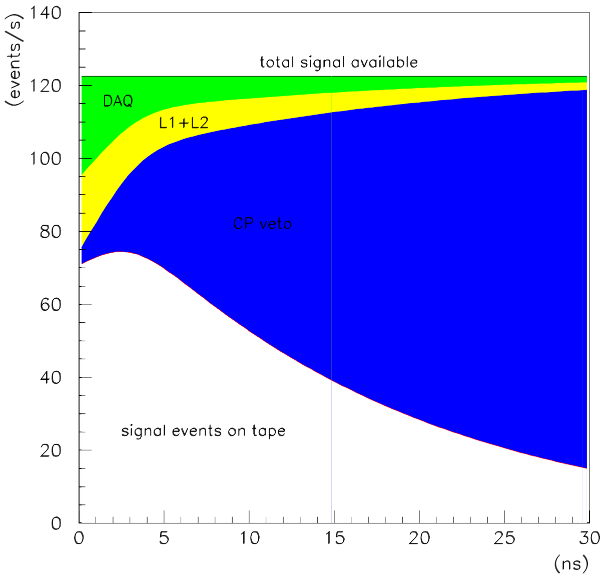

Figure 19: Decomposition of signal losses among various stages of the event pipeline as a function of the width of the CPV veto window t_C at a beam current of 250nA, with the upper-level trigger improvements foreseen for 1999 running in place. The large increases in trigger and data acquisition dead-time at low values of t_C reflect the onset of leakage from charged reactions that enter as the veto efficiency decreases from unity.

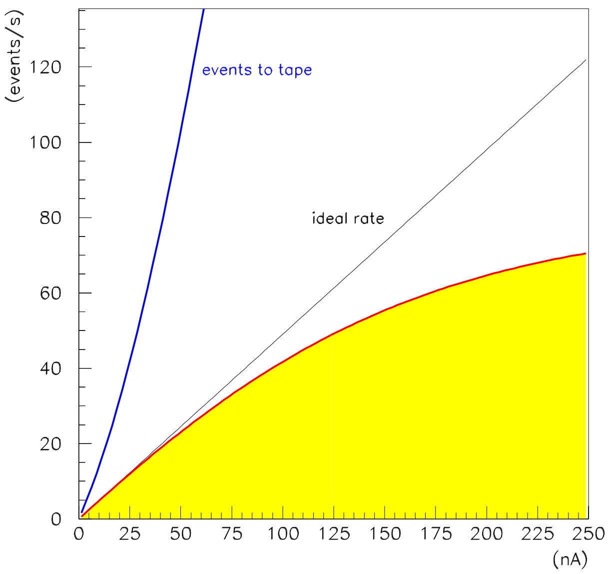

Figure 20: Comparison between ideal and actual rates of recording signal events on tape as a function of beam intensity, under the conditions of a level 1 trigger and improved DAQ, and with the online CPV veto disabled.

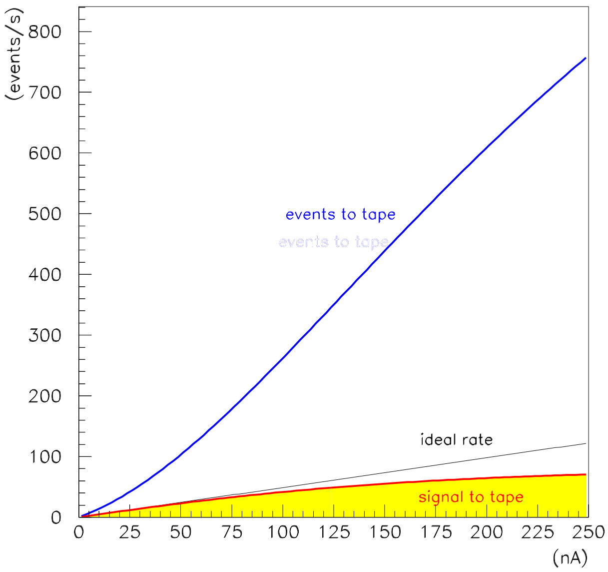

Figure 21: Same as Fig. 20 but with expanded vertical scale.

any data under these conditions. By looking at data with both CPV and UPV vetoes disabled, it is possible to check how many of the events come with a coincident UPV signal and subtract them off, but most of that data sample is completely skewed by the presence of the level 2 trigger condition. Taking what I believe to be reasonable estimates for the inputs that cannot be directly extracted from the data, it is now possible to produce a realistic prediction for the yield of signal events on tape as a function of t_C all the way down to zero CPV window width. The result is shown in Fig. 19. The conclusion from this plot is that the best yield is obtained with no online CPV veto at all!

The fact that we are writing all of this signal to tape does not necessarily mean that it will be possible to recover offline the set of events with accidental CPV hits within the coincidence peak. However the CPV is highly segmented, which makes it possible to recover events with a CPV inside the coincidence region provided that it does not physically overlap with a cluster in the LGD. Hence the expectation is that many of these events will in fact be usable. Fixing $t_C = 0$, the yield of signal events to tape under 1999 conditions, as a function of beam current, is shown in Figs. 20-21. These two are the same figure shown with different vertical scales. It is true that most of the 800 events/s being written to tape at 250nA have charged particles in the forward region. Most of them could be eliminated during a crude one-pass reduction made offline. The most important conclusion of this report is that only by disabling the online CPV veto can Radphi make effective use of 250nA of beam, that corresponds to $5 \cdot 10^7$ tagged photons/s.

2.4 what remains to be done

1. It would be good if we could refine our knowledge of the parameters in Table 2.3 for which the method is listed "guess". It would be possible to measure these if we had a large-statistics sample of minimum-biased events (*i.e.* with a trigger that required only the RPD OR). Unfortunately the run log does not record us having taken any such data during the June run, in particular, without the tagger OR in the trigger. We should think of how these numbers can be extracted from the data we have.

2. Whether it is applied online or offline, an efficient CP veto is extremely important to this experiment. A subset of the phototubes on the CPV counters showed evidence of saturation at beam intensities that still lower than what is foreseen for 1999 running. Perhaps the advent of a higher energy beam will decrease the overall rates in the CPV, but whether there will be a substantial decrease we cannot be certain. We should be sure that the counters that cover the region close to the beam axis are equipped with bases that are capable of efficient operation at 5MHz.

Table 2: Input parameters to the model for 1999 running conditions, together with information about how the value for the parameter was obtained.

parameter	value		method
r_{T}	$1.94 \cdot 10^{5}$	/s/nA	fit to scaler data
r_{R}	$1.45 \cdot 10^{3}$	/s/nA	fit to scaler data
r_{U}	$1.4 \cdot 10^{4}$	/s/nA	fit to scaler data
r_{C}	$2.7 \cdot 10^{5}$	/s/nA	fit to scaler data
t_{T}	$1.0 \cdot 10^{-8}$	s	to be chosen
t_{U}	$1.5 \cdot 10^{-8}$	s	to be chosen
t_{C}	0	s	no CPV in trigger
σ_{C}	$2.6 \cdot 10^{-9}$	s	measured with UPV OR tdc
d_{T}	$1.0 \cdot 10^{-8}$	s	fit to scaler data
d_{C}	$1.0 \cdot 10^{-8}$	s	fit to scaler data
d_1	$1.2 \cdot 10^{-6}$	s	fast-clear specifications
d_2	$1.4 \cdot 10^{-5}$	s	measured on scope
d_{DAQ}	$3.0 \cdot 10^{-4}$	s	promised by DAQ gurus
$f_{T\not{C}\not{V}}$	$2.6 \cdot 10^{-3}$		measured at low rate
$f_{\not{T}\not{C}\not{V}}$	$5.5 \cdot 10^{-1}$		measured with veto in/out
$f_{TC\not{V}}$	$5.0 \cdot 10^{-3}$		pure guess (should be small)
$f_{\not{T}C\not{V}}$	$2.2 \cdot 10^{-1}$		reasonable guess
$f_{1_{T\not{C}\not{V}}}$	1.0		conservative estimate
$f_{1_{\not{T}\not{C}\not{V}}}$	$3.0 \cdot 10^{-2}$		reasonable guess
$f_{1_{TC\not{V}}}$	1.0		conservative estimate
$f_{1_{\not{T}C\not{V}}}$	$2.0 \cdot 10^{-1}$		reasonable guess
$f_{2_{T\not{C}\not{V}}}$	$1.3 \cdot 10^{-1}$		fit to scaler data
$f_{2_{\not{T}\not{C}\not{V}}}$	$3.5 \cdot 10^{-3}$		fit to scaler data
$f_{2_{TC\not{V}}}$	$1.0 \cdot 10^{-1}$		reasonable guess
$f_{2_{\not{T}C\not{V}}}$	$2.5 \cdot 10^{-2}$		reasonable guess

3. At present the UPV counters have been mounted with a 10cm x 10cm inner square hole for the beam. If the CPV is removed as an online veto then it is incumbent on the UPV signal to remove as much as possible of the background in the RPD OR associated with photon beam halo. The aperture of the UPV should be decreased to intercept as much of the beam halo as possible, without going so far that the UPV rate begins to introduce random vetoes as a significant level. Monte Carlo indicates that with the current shielding configuration the UPV OR rate would not exceed 20KHz/nA if the aperture were decreased to match that of the CPV. This would provide a better shield from upstream backgrounds than we presently have, and at the same time not introduce significant additional losses. Background from upstream conversions is especially important when CLAS is running, and the UPV helps to reduce our sensitivity to the presence of their target.

4. With a minor adjustment it should be possible to reduce the adc gate width from its present value of 250ns. At some point, reducing the gate width further results in a loss of energy resolution as one cuts into the tail of the pulse. On the other hand, anything from an interaction within the duration of the gate, other than what caused the trigger, that creates a signal in the lead glass will corrupt the event and in most cases effectively remove it from our sample. This amounts to another dead-time effect in the electronics, and we need to understand its impact at the same level we have understood the trigger. This will require a Monte Carlo study with **Gradphi**[2].

5. During 1998 running there was an unexpected failure mode in the adc modules which caused clusters of adjacent channels to generate anomalously large adc values. These blocks were effectively removed from active use by encoding their row,column addresses to values outside the range subtended by the LGD. However they add considerable overhead to the level 2 processing time, which had an adverse effect on dead-time. We would like to understand this problem, or at least have sufficient spares available to replace failed channels during 1999.

6. During 1998 running, the zero-suppression feature of the adc modules was disabled so that every adc in the crate produced a data word in the event for every event. This generates unnecessary overhead both in DAQ dead-time and disk space. Anticipating a much higher event rate for 1999 running, we should switch over to use zero suppression.

7. In order to have the possibility of running at design intensity in 1999 we must have the new level 1 trigger installed and working.

References

[1] K. Burchesky and E. Smith, "Study of Thresholds in the Pb glass in a Level 1 Trigger", *Radphi Technical Note 1998-257*.

[2] **Gradphi** is a Monte Carlo simulation of the Radphi apparatus and beam line that was developed by A. Kurylov and others. It is ready and available for use under the CVS software repository for this experiment.